Transcellular delivery of vesicular SOCS proteins from macrophages to epithelial cells blunts inflammatory signaling

Emilie Bourdonnay,[1] Zbigniew Zasłona,[1] Loka Raghu Kumar Penke,[1] Jennifer M. Speth,[1] Daniel J. Schneider,[1] Sally Przybranowski,[1] Joel A. Swanson,[2] Peter Mancuso,[3] Christine M. Freeman,[1,4] Jeffrey L. Curtis,[1,5] and Marc Peters-Golden[1]

[1]Division of Pulmonary and Critical Care Medicine, Department of Internal Medicine and [2]Department of Microbiology and Immunology, University of Michigan Medical School; and [3]Department of Environmental Health Sciences, School of Public Health; University of Michigan, Ann Arbor, MI 48109
[4]Research Services and [5]Medical Services, Department of Veterans Affairs Health Care System, Ann Arbor, MI 48105

JAK–STAT signaling mediates the actions of numerous cytokines and growth factors, and its endogenous brake is the family of SOCS proteins. Consistent with their intracellular roles, SOCS proteins have never been identified in the extracellular space. Here we report that alveolar macrophages can secrete SOCS1 and –3 in exosomes and microparticles, respectively, for uptake by alveolar epithelial cells and subsequent inhibition of STAT activation. Secretion is tunable and occurs both in vitro and in vivo. SOCS secretion into lung lining fluid was diminished by cigarette smoking in humans and mice. Secretion and transcellular delivery of vesicular SOCS proteins thus represent a new model for the control of inflammatory signaling, which is subject to dysregulation during states of inflammation.

CORRESPONDENCE
Marc Peters-Golden:
petersm@umich.edu

Abbreviations used: Ab, antibody; AEC, alveolar epithelial cell; AM, alveolar macrophage; BALF, bronchoalveolar lavage fluid; CM, conditioned medium; Exo, exosome; MCP-1, monocyte chemotactic protein 1; MP, microparticle; PGE_2, prostaglandin E_2; PM, peritoneal macrophage; PS, phosphatidylserine; qRT-PCR, quantitative RT-PCR; WB, Western blot.

JAK-STAT signaling is critical in transducing the effects of many cytokines, hormones, and growth factors. Upon ligation, receptors for these molecules recruit JAKs, which subsequently phosphorylate tyrosine residues on STATs, transcription factors which then dimerize and translocate to the nucleus and bind specific DNA sequences on target genes. Although most STAT-dependent genes serve proinflammatory functions, a family of STAT-induced STAT inhibitors termed SOCS proteins serves to turn off responses to these same stimuli in a classical negative feedback loop (Yoshimura et al., 2007). The critical braking function of SOCS proteins is illustrated by the hyperinflammatory phenotypes observed when they are deleted or deficient (Tamiya et al., 2011). SOCS1 and -3 are the members of this family that have been best studied and the only ones with a direct ability to inhibit the kinase activity of JAK. Classically, SOCS1 is induced by (Tamiya et al., 2011) and dampens signaling (Starr et al., 1997) via STAT1 in response to IFNγ stimulation, whereas SOCS3 is induced by (Tamiya et al., 2011) and dampens signaling via STAT3 in response to IL-6 (Nicholson et al., 1999). However, substantial overlap exists in the stimulus specificity of individual STATs as well as the target STAT specificity of particular SOCS molecules. Befitting their obligate intracellular role, SOCS proteins have never been identified in the extracellular space.

The pulmonary alveolar surface epitomizes an anatomical site at which homeostasis is severely tested because it is continually exposed to potentially harmful inhaled toxins, antigens, and pathogens, yet must curb overexuberant inflammatory responses to these challenges to safeguard the lung's vital gas exchange function. This vast surface is composed of alveolar epithelial cells (AECs). Though once regarded as inert barrier cells, AECs are now recognized to elaborate an array of proinflammatory and innate immune cytokines and chemokines, both constitutively and in response to inflammatory stimuli (Chuquimia et al., 2012). Alveolar macrophages (AMs) are the resident immune cells of the alveolar surface and have a critical role in

The Rockefeller University Press $30.00
J. Exp. Med. 2015 Vol. 212 No. 5 729–742
www.jem.org/cgi/doi/10.1084/jem.20141675

The Journal of Experimental Medicine

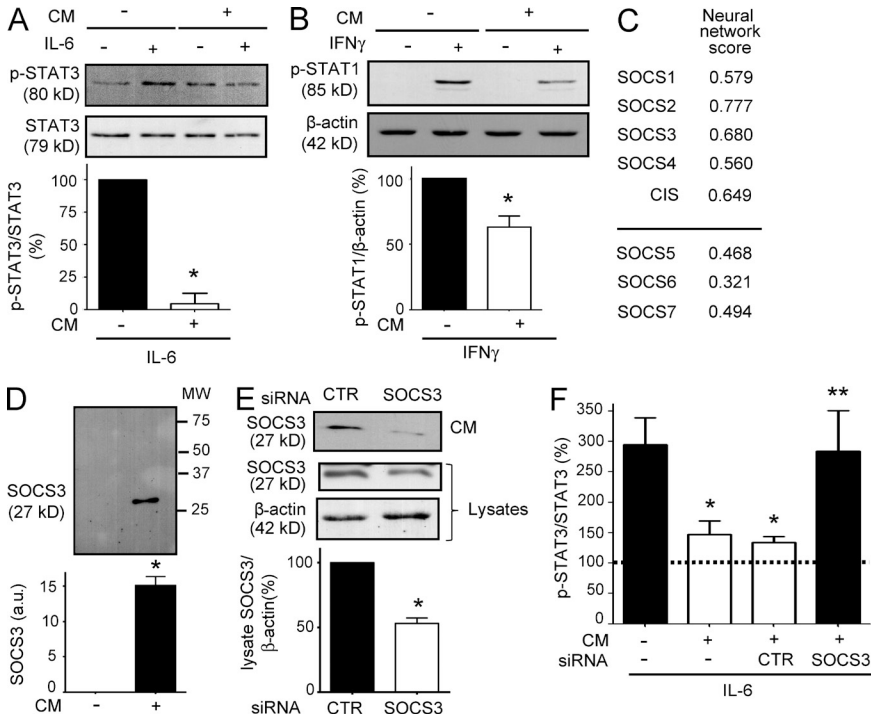

Figure 1. SOCS3 protein mediates inhibition of AEC STAT activation by AM-derived CM. (A and B) AECs were incubated for 2 h with medium alone (−) or CM obtained from AMs cultured overnight (+) and challenged for 1 h with 20 ng/ml IL-6 (A) or 5 ng/ml IFNγ (B), and lysates were analyzed for p-STAT3 (A) or p-STAT1 (B); activation is expressed as a percentage of the level of p-STAT3 (normalized to total STAT3) or p-STAT1 (normalized to β-actin) measured in cytokine-treated cells not pretreated with CM. (C) SecretomeP 2.0–derived neural network scores for SOCS family members; those with scores >0.5 are predicted to be unconventionally secreted. (D) Overnight AM CM (+) or RPMI 1640 alone (−) were concentrated and subjected to WB analysis for SOCS3; bar graph depicts arbitrary densitometric units of SOCS3. (E) Cell lysates and CM from AMs incubated with nontargeting control (CTR) or SOCS3 siRNA were analyzed for SOCS3 protein by WB; representative blots are shown at top, and mean lysate data are shown below. (F) AECs were incubated for 2 h with overnight CM obtained from untreated or CTR siRNA– or SOCS3 siRNA–treated AMs and then challenged with IL-6. STAT3 activation was assessed by determining phospho-STAT3 levels by WB; values in F represent the percentage of STAT3 activation present in unstimulated cells, which is indicated by the dashed line. (A, B, and D–F) Data represent the mean ± SE from at least three independent experiments. *, $P < 0.05$ versus cytokine-treated AECs pretreated with medium alone (A, B, and F) or RPMI 1640 alone (D) or versus CTR siRNA–treated AMs (E); **, $P < 0.05$ versus IL-6–treated AECs pretreated with CM from AMs treated with CTR siRNA (F).

lung host defense. Resident AMs at baseline have long been recognized to manifest a more quiescent and suppressive phenotype than that of other tissue macrophages (Thepen et al., 1994) or precursor monocytes. This unusual macrophage phenotype has been largely attributed to conditioning by AEC-derived substances, including surfactant protein A, transforming growth factor-β, IL-10, and prostaglandin E_2 (PGE_2; Hussell and Bell, 2014). Morphometric (Hyde et al., 2004) and live confocal microscopy (Westphalen et al., 2014) studies demonstrate an abundance of less than one AM per alveolus in the normal mammalian lung. Moreover, and contrary to longstanding assumptions, AMs have recently been reported to be sessile (Westphalen et al., 2014). These observations imply that paracrine actions of AMs likely represent an important means of communication with neighboring AECs. Although stimulatory effects of AM-derived mediators on AEC chemokine expression (Standiford et al., 1990) and proliferation (Brandes and Finkelstein, 1989) are recognized, little is known about the ability of AMs to secrete mediators that restrain inflammatory signaling or responses by AECs.

We therefore investigated the ability of products secreted by AMs to attenuate JAK-STAT signaling in AECs. Unexpectedly, we found that AMs secrete SOCS1 and SOCS3 proteins in vesicles that can be taken up by AECs to mediate inhibition of cytokine-induced STAT activation. This secretion occurs both in vitro and in vivo, is a tunable phenomenon, and can be dysregulated during inflammation. These findings reveal a previously unappreciated means for intercellular communication in inflammation control.

RESULTS

SOCS3 protein mediates inhibition of AEC STAT activation by AM-derived conditioned medium (CM)

CM was collected from primary rat AMs, which had been adhered and cultured overnight, and centrifuged at 500 *g* (to remove floating cells) and 2,500 *g* (to remove debris and apoptotic bodies). To assess its immunoregulatory capacity, CM was added to rat L2 AECs 2 h before addition of proinflammatory cytokines. As compared with RPMI 1640 alone, AM-derived CM inhibited IL-6–induced activation of STAT3 (indicated by phosphorylation on Tyr 705; Fig. 1 A) as well as IFNγ-induced activation of STAT1 (indicated by phosphorylation on Tyr 701; Fig. 1 B); these effects were confirmed using RLE-6TN, another nontransformed rat AEC line (not depicted). To address the possibility that this inhibition of STAT activation might be attributable to increased expression of endogenous SOCS protein in response to treatment with the cytokine itself, we tested the effect of a 1-h incubation with IL-6 on levels of SOCS3 protein determined by Western blot (WB) analysis in lysates of AECs. These data (not depicted) demonstrated no meaningful increase in endogenous

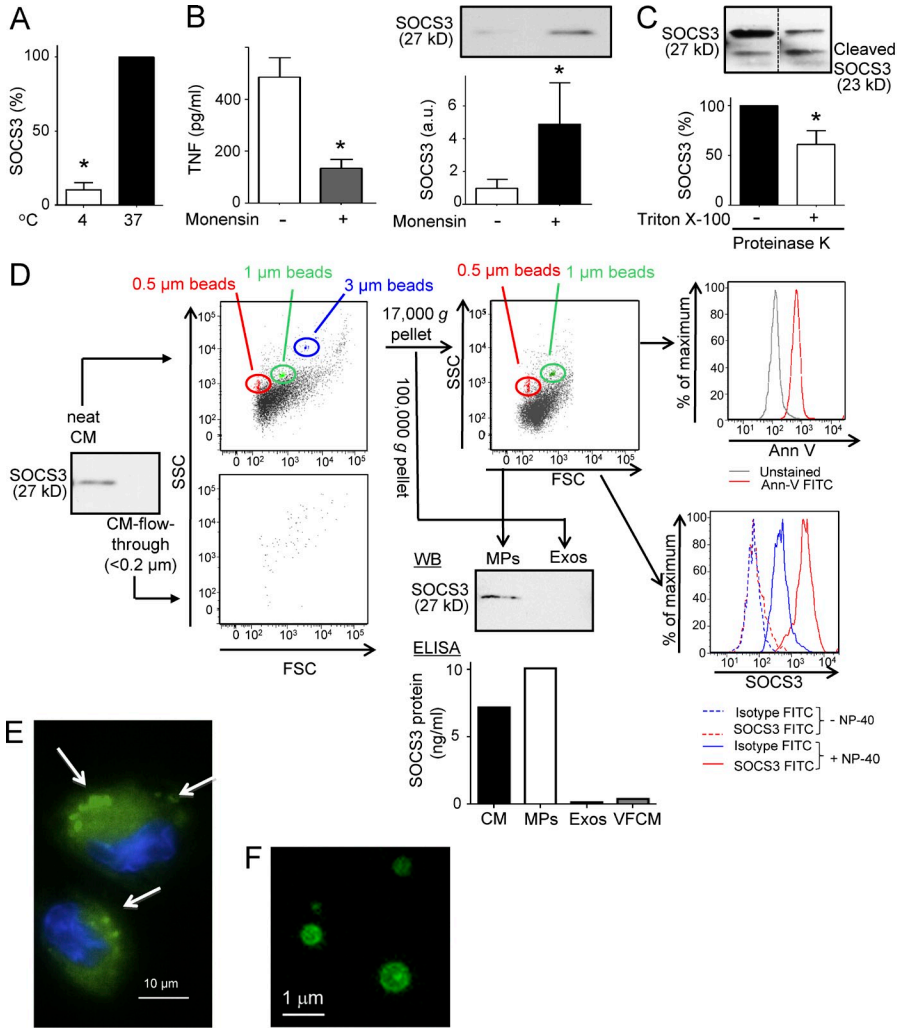

Figure 2. SOCS3 secretion by AMs proceeds via an unconventional vesicular pathway and mainly involves MPs. (A) AMs were adhered and cultured for 1 h at 37°C or at 4°C. Then CM was concentrated and subjected to WB analysis for SOCS3. SOCS3 levels in CM are expressed as the percentage of SOCS3 secreted by AMs kept at 37°C. (B) AMs were treated with 1 µM monensin for 1 h, after which CM was harvested for determination of TNF by ELISA (left) or concentrated and subjected to WB analysis for SOCS3 (right). SOCS3 levels in CM are expressed as arbitrary densitometric units. (C) CM was obtained from AMs after 1-h adherence, concentrated, and incubated for 2 h with 0.1 mg/ml proteinase K in the presence or absence of 1% Triton X-100 and then analyzed by WB for SOCS3. SOCS3 is expressed as the percentage of that measured in nondetergent-treated CM. The dashed vertical line separates lanes that were loaded on the same gel but were not contiguous. (D) Neat CM and the flow through from a 0.2-µm filter were concentrated and subjected to either WB for SOCS3 or analysis by flow cytometry. Particles were further subjected to size determination using standard beads of known size. Additionally, MPs and Exos were purified from CM by differential centrifugation and subjected to WB for SOCS3. MPs were further analyzed for staining with FITC–annexin V and FITC–anti-SOCS3 with (continuous line) or without (dashed line) pretreatment with 0.2% NP-40. Additionally, whole CM, MPs, Exos, and vesicle-free CM (VFCM) were collected and then subjected to SOCS3 quantitation by ELISA (bottom graph). (E) AM plasma membranes were labeled by incubating cells on ice in the dark for 20 min with 100 µM of the fluorescent lipid 18:1-06:0 NBD PC (green) and counterstained with DAPI; then cells were washed twice with PBS and plated for 1 h, and MP budding was assessed by fluorescence microscopy using an Eclipse E600 microscope and 100 magnification; arrows indicate membrane blebs. (F) The MP pellet from AM CM was incubated with FITC–annexin V in the dark and imaged on a TE300 with a 60× oil immersion objective (NA 1.40, total magnification of 600). Data in A–D (except for ELISA data which are from a single experiment representative of two) represent the mean ± SE from at least three independent experiments; data in E and F are representative of two independent experiments. *, $P < 0.05$ versus 4°C cells (A), untreated cells (B), or CM untreated with 1% Triton X-100 (C).

SOCS3 protein expression within this short time frame, instead pointing to the actions of an inhibitory molecule in AM CM.

We considered the possibility that the inhibitor of STAT activation in AM-derived CM might be a SOCS protein. Although members of the SOCS family have never previously been identified extracellularly, informatics analysis supported the plausibility of SOCS secretion. Although SOCS1 and SOCS3 lack an N-terminal leader sequence typical of proteins secreted via conventional ER–Golgi pathways (Bendtsen et al., 2004b), both are among those SOCS family members meeting prediction criteria (SecretomeP 2.0–derived neural network score >0.5; Bendtsen et al., 2004a) for secretion by unconventional pathways (Fig. 1 C), a phenomenon now well recognized for "leaderless" proteins (Nickel and Rabouille, 2009). In view of its higher neural network score, we initially assessed the presence of SOCS3 in concentrated AM-derived CM by performing WB analysis. This revealed a single band at the expected molecular weight for SOCS3 (Fig. 1 D).

To confirm the identity of this band as the product of the SOCS3 gene, we verified that its level declined substantially in CM obtained from AMs treated with SOCS3 siRNA as compared with that obtained from AMs treated with control scrambled siRNA (Fig. 1 E). We next assessed the ability of CM from AMs in which SOCS3 expression had been knocked down to inhibit activation of STATs. CM from AMs treated with SOCS3 siRNA, but not control siRNA, lost its ability to inhibit AEC STAT3 activation in response to IL-6 (Fig. 1 F), as well as STAT1 activation in response to IFNγ (not shown). Although STAT activation can also be negatively regulated

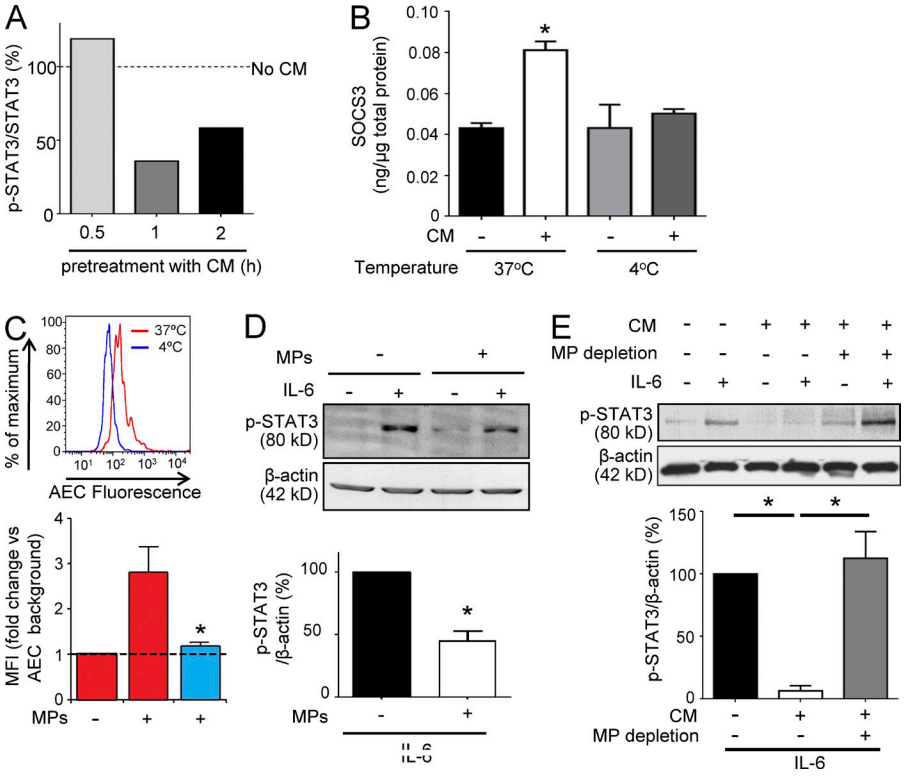

Figure 3. Uptake of SOCS3-containing MPs by AECs inhibits target cell STAT3 activation. (A) AECs were pretreated with CM from AMs cultured overnight for the time intervals indicated, after which they were challenged with IL-6 for 1 h and lysates were subjected to WB for STAT3 activation; results are expressed as the percentage of the stimulated increase in cytokine-treated cells not receiving AM CM, indicated by the dashed line. (B) AECs were treated with or without AM CM for 2 h at 37°C or at 4°C, after which AEC lysate proteins were subjected to SOCS3 quantitation by ELISA. Data are expressed as ng/µg of total protein. (C) AM-derived MPs were labeled with FITC–annexin V and added to AECs at a ratio of 10:1 for 1 h at 37°C or at 4°C. Increases in fluorescence in AEC cultures were determined by flow cytometry and are depicted as histograms from a representative experiment (top) and mean fluorescence intensity (MFI; fold change versus background fluorescence of AECs alone) from three experiments (bottom). MFI of AECs receiving FITC–annexin V without MPs at 37°C was similar to background (not depicted). (D) MPs isolated from AM CM were incubated with AECs at a ratio of 10:1 for 2 h before stimulation with IL-6, and lysates were analyzed for STAT3 activation and expressed as the percentage of that determined in cytokine-treated AECs not pretreated with MPs. (E) AECs were pretreated with or without CM or with MP-depleted CM for 2 h at 37°C before stimulation with IL-6, after which lysates were analyzed for STAT3 activation and expressed as the percentage of that determined in cytokine-treated AECs not pretreated with CM. (A–E) Data represent the mean ± SE from at least three independent experiments (B–E) or are representative of two independent experiments (A). *, $P < 0.05$ versus AECs not pretreated with CM at 37°C (B), AECs incubated with FITC–annexin V–labeled MPs at 37°C (C), cytokine-stimulated AECs not pretreated with MPs (D), or AECs pretreated with CM (E).

by tyrosine phosphatases SHP1 and SHP2, these phosphatases are not predicted by SecretomeP 2.0 to be unconventionally secreted.

SOCS3 secretion by AMs proceeds via an unconventional vesicular pathway mainly involving microparticles (MPs)

We found SOCS3 secretion to be unassociated with LDH release (not depicted), arguing against it being a manifestation of cytotoxicity. In addition, it was markedly reduced at 4°C, suggesting that it is an energy-dependent phenomenon (Fig. 2 A). To confirm that SOCS3 is indeed released by AMs through unconventional secretion, we tested the effects of monensin, an inhibitor of conventional secretion. As expected, monensin inhibited rat AM secretion of the known conventionally secreted protein TNF (Fig. 2 B, left); in contrast, it increased secretion of SOCS3 (Fig. 2 B, right), as it has previously been recognized to do for other unconventionally secreted proteins (Rubartelli et al., 1990). Similar results were obtained using brefeldin A, another inhibitor of conventional secretion (not depicted). Unconventional secretion can be vesicular in nature; the finding that SOCS3 in AM-derived CM was more sensitive to proteolysis in the presence of a detergent (Fig. 2 C) implied its packaging within a membranous structure, such as an extracellular vesicle.

The two main types of extracellular vesicles capable of harboring protein cargo are MPs and exosomes (Exos). MPs (also known as microvesicles or ectosomes) originate by budding or shedding from the plasma membrane, are between 0.1 and 1 µm in diameter, and are annexin V positive, owing to the phosphatidylserine (PS) on their outer surface (Hugel et al., 2005). In contrast, Exos originate from endosomal membranes and are <0.1 µm in diameter. To better characterize the type of vesicles containing SOCS3, we passed AM CM through a 0.2-µm filter, which separates MPs from Exos contained in the flow through. The neat CM was verified to contain SOCS3 (by WB) as well as MPs, as indicated by flow cytometric demonstration of a population of particles with a diameter of 0.5–1 µm that were largely annexin V positive, whereas the flow through contained neither SOCS3 nor MPs (Fig. 2 D). MPs budding from AMs could be visualized directly by fluorescence microscopy after labeling the plasma membranes of cells in suspension with the fluorescent lipid 18:1-06:0 NBD PC before plating (Fig. 2 E). To confirm

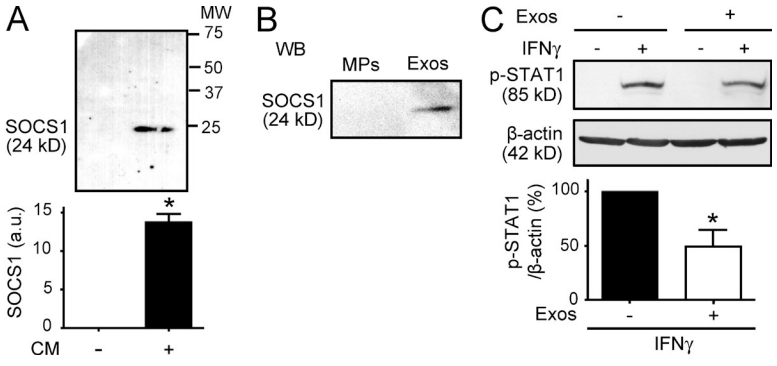

Figure 4. SOCS1 protein is secreted in Exos and exerts inhibitory effects on AEC STAT1 activation. (A) Overnight AM CM (+) or RPMI 1640 alone (−) was concentrated and subjected to WB analysis for SOCS1; bar graph depicts arbitrary densitometric units of SOCS1. (B) MPs and Exos were isolated from overnight CM and subjected to WB for SOCS1. (C) AECs were pretreated for 2 h with (+) Exos isolated from overnight CM or with RPMI 1640 alone (−) before a 1-h stimulation with IFNγ, after which AEC lysate proteins were subjected to immunoblot analysis for p-STAT1. STAT1 activation was expressed as the percentage of p-STAT1, normalized for β-actin, in cytokine-treated AECs not pretreated with AM-derived Exos. (A–C) Data represent the mean ± SE from at least three independent experiments (A and C) or are representative of two independent experiments (B). *, $P < 0.05$ versus RPMI 1640 alone (A) or IFNγ-treated AECs not treated with Exos (C).

that SOCS3 is in MPs, they were isolated from CM by centrifugation at 17,000 *g* (Brogan et al., 2004). The presence of MPs in this pellet was verified by visualizing annexin V–positive vesicles of varying sizes by fluorescence microscopy (Fig. 2 F), and this MP fraction also contained SOCS3 protein, as determined by WB analysis and by a commercially available ELISA (Fig. 2 D). The presence of SOCS3 within these MPs was further confirmed by their flow cytometric positivity when stained with a fluorochrome-conjugated anti-SOCS3 antibody (Ab; different from that used for WB analysis) with, but not without, membrane permeabilization by gentle detergent treatment using NP-40 (Fig. 2 D). Of note, Exos, pelleted by 100,000 *g* centrifugation of the 17,000 *g* supernatant, contained no SOCS3, as determined by either WB or ELISA; ELISA also verified the absence of SOCS3 in CM depleted of both types of vesicles (Fig. 2 D).

Uptake of SOCS3-containing MPs by AECs inhibits target cell STAT3 activation

The known ability of vesicles to be internalized via either membrane fusion or endocytosis (Mause and Weber, 2010) could explain the antiinflammatory actions in target AECs of SOCS-containing vesicles released by AMs. Indeed, the duration of AEC pretreatment with AM CM required to attenuate subsequent STAT3 activation (>30 min, maximal by 60 min; Fig. 3 A) is consistent with the time frame that has been previously established for vesicular uptake (Sadallah et al., 2008). To directly evaluate the uptake of AM-derived SOCS3 by AECs, ELISA was used to quantify intracellular levels of SOCS3 in lysates of AECs prepared before and after a 2-h incubation with AM CM. Baseline intracellular SOCS3 levels doubled after incubation with CM at 37°C but remained unchanged after incubation at 4°C ($n = 3$; Fig. 3 B). In parallel fashion, AECs incubated at 37°C with FITC–annexin V–labeled, AM-derived MPs exhibited an increase in fluorescence as determined by flow cytometry, whereas incubation at 4°C resulted in no such increase (Fig. 3 C). Together these data demonstrate energy-dependent uptake by AECs of AM-derived MPs as well as SOCS3. Because SOCS3 was enriched within AM-derived MPs and these MPs could be taken up by AECs, we next tested the ability of purified MPs to reproduce the anti-inflammatory actions of neat AM CM on AECs. MPs, added at a commonly used ratio of 10 MPs to 1 target cell (Gasser et al., 2003), were indeed capable of inhibiting IL-6–induced STAT3 activation in AECs (Fig. 3 D). In reciprocal fashion, AM CM lost its ability to inhibit AEC STAT3 activation after depletion of MPs by centrifugation at 17,000 *g* (Fig. 3 E).

SOCS1 protein is secreted in Exos and exerts inhibitory effects on AEC STAT1 activation

Because SOCS1 was also predicted to be secreted (Fig. 1 C), we evaluated its presence in AM CM using WB. It too was identified as a single band at the appropriate molecular weight (Fig. 4 A). However, differential centrifugation revealed SOCS1 to be present primarily in the Exos fraction (pellet obtained from 100,000 *g* centrifugation of the 17,000 *g* supernatant; Fig. 4 B), rather than in the MP fraction, as was the case with SOCS3 (Fig. 2 D). Consistent with this finding, flow cytometric staining of MPs using FITC-conjugated anti-SOCS1 after gentle detergent permeabilization was negative (not depicted). As shown for MPs (Fig. 3 D), the functional activity of AM-derived Exos was confirmed by their ability to inhibit IFNγ-induced STAT1 activation in AECs (Fig. 4 C). Moreover, the ability of AM CM to inhibit IFNγ-induced STAT1 activation was attenuated by pretreatment of AMs with SOCS1 siRNA (not depicted). Together, these data indicate that SOCS1 contained in Exos abrogates STAT1 activation.

SOCS3 secretion is a regulated phenomenon in vitro

Macrophage adherence to plastic culture dishes is recognized to trigger a burst of activation (Kelley et al., 1987). We found that adherence resulted in a rapid burst of release of both SOCS3 (Fig. 5 A, top) as well as MPs (quantified by flow cytometry; Fig. 5 A, bottom), followed by a much lower basal rate of secretion after adherence. SOCS3 secretion increased as early as 5 min after AM adherence (Fig. 5 B). The rapidity of this response is consistent with the known kinetics of MP release described for monocytes (MacKenzie et al., 2001). We next sought to determine whether AM secretion of SOCS proteins could be regulated by known immunomodulatory

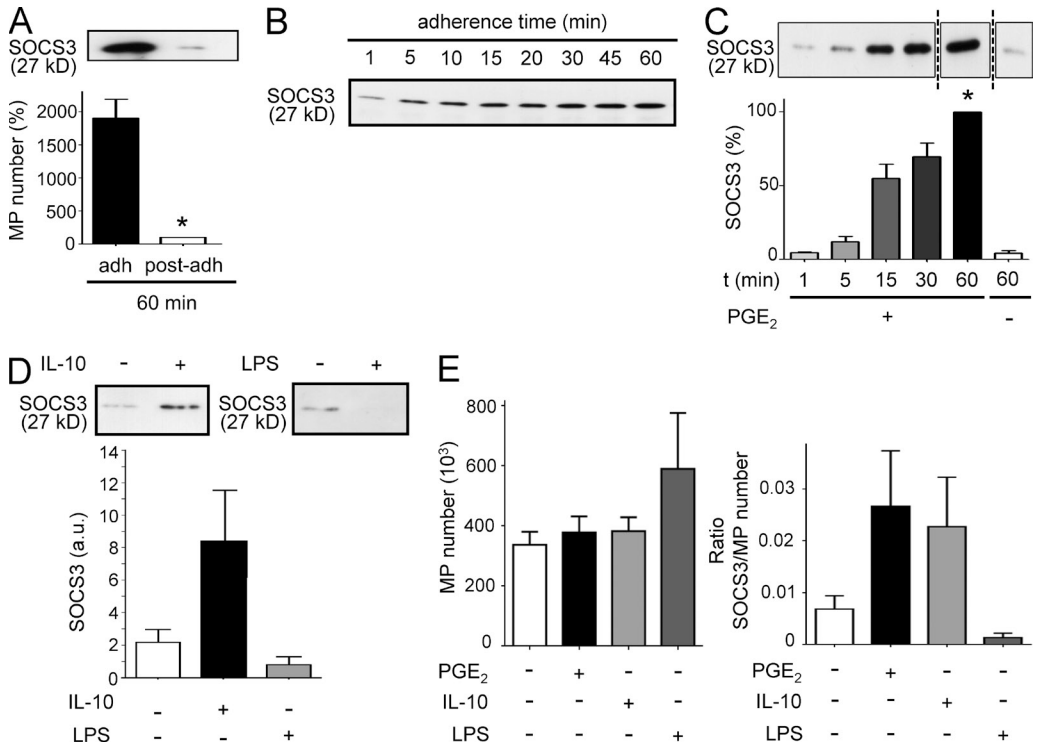

Figure 5. SOCS3 secretion is a regulated phenomenon in vitro. (A) AMs were adhered to tissue culture plates for 60 min (adh) and then cultured for another 60 min after changing the medium (post-adh); SOCS3 in concentrated CM was analyzed by WB (top), and MP number was assessed by flow cytometry (bottom) and expressed as the percentage of the number quantified in 60-min post-adh CM. (B) AMs were adhered for the time intervals shown, and SOCS3 in concentrated CM was determined by WB. (C and D) Post-adh AMs were treated either with 1 µM PGE_2 for the times indicated (C) or with 10 ng/ml IL-10 or 5 µg/ml LPS for 1 h (D), after which CM was concentrated and SOCS3 determined. SOCS3 levels are expressed as the percentage of SOCS3 secreted after 60-min treatment with PGE_2 (C) or as arbitrary densitometric units (D). The dashed vertical lines in C separate lanes on the same gel that were not contiguous. (E) Post-adh AMs were treated for 1 h with PGE_2, IL-10, or LPS at the doses noted above; MP number in CM was assessed by flow cytometry (left) and the ratio of SOCS3 (determined by WB)/MP number is indicated (right). (A–E) Data represent the mean ± SE from at least three independent experiments (A and C–E), or the blot shown is representative of two experiments (B). *, $P < 0.05$ versus adh AMs (A) or untreated AMs (C).

molecules. The lipid mediator PGE_2 down-regulates many features of AM activation (Aronoff et al., 2004; Bourdonnay et al., 2012), and the cytokine IL-10 is well known for its antiinflammatory and immunosuppressive actions (Sabat et al., 2010); these are of particular interest because both are known to be secreted by AECs (Chauncey et al., 1988; Jose et al., 2009) and thus could potentially mediate communication from AECs to AMs. Both rapidly potentiated basal secretion of SOCS3 when added during the post-adherence phase (Fig. 5, C and D), and PGE_2 also increased secretion of SOCS1 (not depicted). In contrast, the proinflammatory endotoxin LPS decreased basal SOCS3 secretion in AMs (Fig. 5 D). Unlike the effects of cell adherence (Fig. 5 A), the ability of these immunomodulatory substances to rapidly increase (IL-10 and PGE_2) or decrease (LPS) SOCS3 secretion by cultured AMs was unassociated with changes in the number of MPs secreted (Fig. 5 E, left), indicating instead an alteration in the content of SOCS packaged per MP (Fig. 5 E, right).

Expression and secretion of SOCS3 by various cell populations

As described for rat AMs, we also found robust secretion of SOCS3 and SOCS1 proteins by resident AMs obtained from healthy human subjects (Fig. 6 A), as well as SOCS3 from mouse AMs (Fig. 6 B, top). Secretion of both SOCS proteins was similarly observed in cell lines derived from primary rat (NR8383 line) and mouse (MH-S line) AMs (not depicted). In contrast, analysis of CM derived from cultured peritoneal macrophages (PMs) from mice (Fig. 6 B, top) and rats (Fig. 6 C, left, top) revealed no appreciable SOCS3, and no SOCS3 was identified by flow cytometry within permeabilized MPs isolated from rat PM-derived CM (Fig. 6 C, bottom); notably, they also expressed very little intracellular SOCS3 (Fig. 6, B [bottom] and C [left, bottom]). Macrophages isolated from mouse spleen as well as phorbol ester–differentiated U937 human monocyte-like cells likewise exhibited minimal degrees of SOCS3 secretion and expression (not depicted). However, SOCS3 was expressed and secreted by rat bone marrow–derived macrophages (Fig. 6 D), implying that this phenomenon is not limited to the lungs. In contrast to the apparent correlation between expression and secretion observed in macrophages (Fig. 6, B and C), normal human lung fibroblasts expressed abundant levels of SOCS3 but failed to secrete it (Fig. 6 E). These data show that abundant intracellular expression of SOCS proteins is necessary but not sufficient

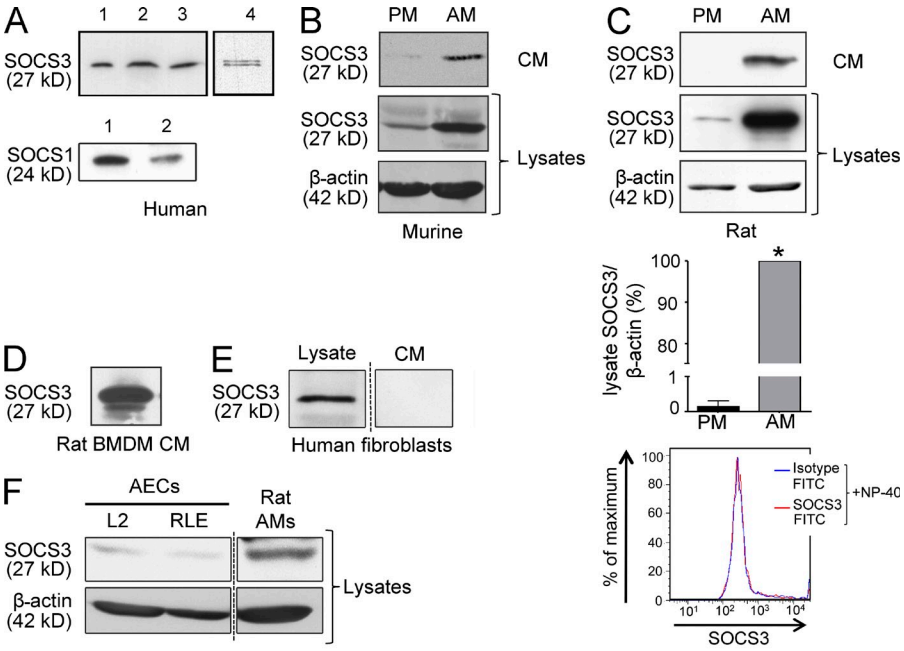

Figure 6. Expression and secretion of SOCS3 by various cell populations. (A) AMs obtained by BAL from normal human subjects were adhered and cultured for 1 h, and concentrated CM was analyzed by WB for SOCS3 ($n = 4$; top) and SOCS1 ($n = 2$; bottom); each lane represents an individual subject. (B) AMs and PMs from a single mouse were cultured overnight, and SOCS3 was determined by WB in concentrated CM and cell lysates. (C) AMs and PMs from a single rat were cultured overnight, and SOCS3 was determined by WB in concentrated CM and cell lysates (top); data in the graph are for lysate values and are expressed as a percentage of the level of SOCS3 (normalized to β-actin) measured in AMs; MPs were isolated from PM-derived CM and analyzed for SOCS3 staining after permeabilization with 0.2% NP-40 (bottom). Error bars indicate SE. (D) Bone marrow–derived macrophages obtained by in vitro differentiation of rat bone marrow cells for 6 d were re-adhered, their medium replaced, and CM obtained after culture for an additional 1 h; SOCS3 was analyzed after concentration of CM. (E) CCL-210 normal human lung fibroblasts were plated for 24 h, the medium changed, and subsequently cultured for an additional 24 h, after which cell lysates and concentrated CM were subjected to WB analysis for SOCS3. (F) Rat AEC lines L2 and RLE-6TN as well as rat AMs were cultured for 16 h. Lysates were analyzed by WB for SOCS3. (E and F) The dashed vertical lines separate lanes that were on the same gel but were not contiguous. (A–F) Data are representative of results from three independent experiments (A and C), or the blot shown is representative of two experiments (B and D–F). *, $P < 0.05$ versus untreated PMs.

for their secretion and confirm that secretion of SOCS proteins is an independently regulated event, consistent with the findings in Fig. 5. Notably, AECs themselves expressed negligible levels of intracellular SOCS3 protein (Fig. 6 F), indicating the possible importance of them acquiring biologically active SOCS3 from donor AMs instead.

Effects of AM-derived SOCS3 on pulmonary STAT activation in vivo

We tested the in vivo ability of AM-derived SOCS3 to influence pulmonary inflammatory signaling by the direct intrapulmonary administration of MPs, using as negative controls MPs that lacked SOCS3. We took advantage of the fact that SOCS3 protein exhibits 100% similarity between rat and mouse by using rat AMs as a source of MPs and normal C57BL/6 mice as recipients. IFNγ activates not only STAT1 but also STAT3 (Qing and Stark, 2004). Intrapulmonary pretreatment with $\sim 3 \times 10^6$ MPs/mouse inhibited IFNγ-induced STAT1 activation (Fig. 7 A), STAT3 activation (Fig. 7 B), and mRNA expression of the STAT-dependent chemokine monocyte chemotactic protein 1 (MCP-1, or CCL2; Fig. 7 C) in lung homogenates depleted of AMs by lavage just before harvest. Interestingly, no corresponding inhibition of STAT1 activation was noted in the lavaged AMs themselves (Fig. 7 D), suggesting that AECs were the target cells responsible for the inhibition noted in lung homogenates. That phosphorylated STAT1 was found mainly in AECs of the IFNγ-challenged lung, and that this AEC STAT1 activation was attenuated by prior intrapulmonary administration of AM-derived MPs, was verified by immunohistochemical staining of lung sections for phospho-STAT1 (Fig. 7 E). In contrast to the effects of AM-derived MPs, administration of the same number of rat PM-derived MPs, isolated from CM which lacks SOCS3 (Fig. 6 C), failed to attenuate lung STAT1 activation (Fig. 7 A) and MCP-1 mRNA expression (Fig. 7 C). These negative data for PS-positive but SOCS3-negative, PM-derived MPs exclude the possibility that the antiinflammatory effects of AM-derived MPs can be explained by potential nonspecific antiinflammatory effects attributable to the PS on their surface.

Regulation and dysregulation of SOCS secretion in the lung in vivo

We next asked whether SOCS secretion occurred in the lung in vivo and whether it was a regulated phenomenon, as was observed in vitro. SOCS3 could be readily identified by WB in concentrated bronchoalveolar lavage fluid (BALF) obtained from the lungs of individual naive mice (Fig. 8 A). In fact, quantitation of SOCS3 in sonicated BALF from naive mice ($n = 10$) by ELISA yielded a level of 10.38 ± 0.96 ng/ml, a concentration which substantially exceeds that reported for most cytokines. Furthermore, just as was observed in vitro, the level of SOCS3 in BALF increased and decreased 3 h after intrapulmonary administration of PGE_2 and LPS, respectively, and an intermediate level was observed when they were co-administered (Fig. 8 A).

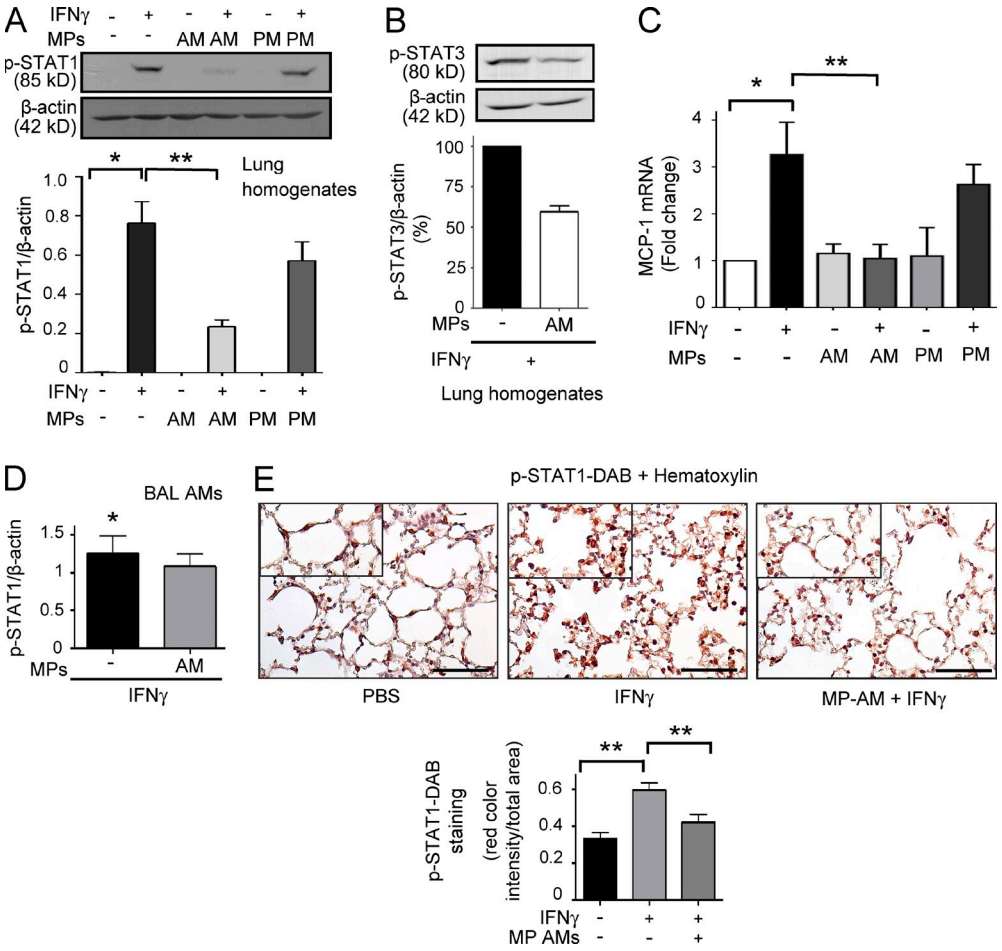

Figure 7. AM-derived SOCS attenuates pulmonary STAT activation in vivo. (A–D) Mouse lungs were pretreated oropharyngeally with 50 µl saline alone or saline containing ∼3 × 10^6 MPs isolated from CM from AMs (A–D) or PMs (A and C). 2 h later, mice received an oropharyngeal dose of 50 µl saline alone or saline containing 0.1 µg IFNγ. 1 h thereafter, their AMs were removed by lavage, and lung homogenates were prepared from the middle right lung for analysis of p-STAT1 (A) and p-STAT3 (B) by WB and from the inferior right lung for analysis of MCP-1 mRNA by qRT-PCR (C). p-STAT1 levels in lysates of lavaged AMs were analyzed by WB (D). (E) Mice were treated with intrapulmonary saline alone or saline containing AM MPs before IFNγ, as in A, and lung sections prepared from the left lung were incubated with hematoxylin to stain nuclei blue and anti-pSTAT1, followed by DAB to stain p-STAT1 red; photographs were taken using an Eclipse E600 microscope (40 magnification), and insets represent enlarged images (top); p-STAT1 staining was quantified by first separating the colors using a color deconvolution plugin (ImageJ software) and performing densitometric analysis of red staining (bottom) in 10 randomly selected fields, which were expressed relative to the area of the whole field. Bars, 500 µm. (A–E) Bar graphs represent the mean ± SE from a minimum of three mice per group in one experiment, which was representative of at least three independent experiments (A, C, and D) or the mean ± SE from 10 randomly selected fields from one representative experiment (E). In B, the blot shown is representative of two independent experiments. *, $P < 0.05$ versus untreated mice (A, C, and D); **, $P < 0.05$ versus IFNγ-treated mice not pretreated with AM-derived MPs (A, C, and E).

As demonstrated in BALF from naive mice (Fig. 8 A), SOCS3 as well as SOCS1 could also be readily identified by WB in BALF obtained by fiberoptic bronchoscopy from healthy, never-smoking human volunteers (Fig. 8 B), consistent with their ex vivo secretion by cultured AMs from these same subjects (Fig. 6 A). It has long been recognized that a chronic state of pulmonary inflammation is elicited by cigarette smoking, which precedes the development of smoking-associated lung disease (Holt, 1987; Cosio et al., 2009). We therefore evaluated levels of both SOCS3 (by WB and ELISA) and SOCS1 (by WB) in BALF from seven never smokers and seven current smokers (20 ± 2.8 pack-years) without respiratory symptoms or lung function abnormalities. By WB analysis in a subset of four subjects per group, levels of both SOCS3 and SOCS1 were significantly decreased by ∼65% and 85%, respectively, in the current smokers as compared with the never smokers. Moreover, BALF SOCS3 levels as determined by ELISA were significantly and similarly reduced by ∼65% in the entire group of seven current smokers as compared with the seven never smokers (Fig. 8 B). Typical features of cigarette smoking–associated inflammation are seen in mice after just a few days of cigarette smoke exposure (John et al., 2014). We exposed C57BL/6 mice to mainstream cigarette smoke from standardized research cigarettes as previously described (Phipps et al., 2010) for 2 h/d for either 3 or 7 d. As compared with smoke-unexposed mice, smoke-exposed mice

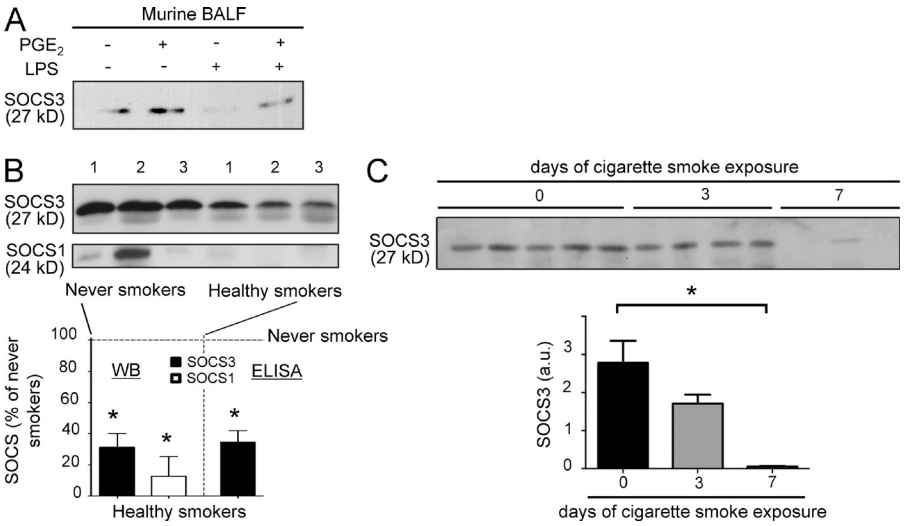

Figure 8. SOCS secretion in the lung in vivo is regulated by immunomodulatory substances and dysregulated in association with cigarette smoking. (A) Mice (three per group) were subjected to intrapulmonary administration of 50 µl saline alone or saline containing 15 µg PGE_2 and/or LPS. BALF was harvested 3 h later, pooled, concentrated, and subjected to WB analysis for SOCS3. (B) BALF from never smokers or healthy current smokers ($n = 4$ subjects per group) was concentrated and subjected to WB analysis for SOCS3 and SOCS1; results from three subjects per group are depicted, with each lane representing an individual subject (top); after densitometric analysis of blots from all four subjects per group, SOCS levels in BALF of smokers was expressed as a percentage of that in never smokers (bottom, left). SOCS3 levels were also determined by ELISA of sonicated BALF in $n = 7$ subjects per group (bottom, right); the mean level in never smokers was 0.26 ± 0.12 pg/µg protein, and that in smokers was expressed as a percentage of the never-smoker level. Error bars indicate SE. (C) Mice were subjected or not to 2 h/d of cigarette smoke for 3 or 7 d, and BALF from at least three mice in each group (as indicated by the individual lanes) was subjected to WB analysis for SOCS3; data at the bottom represent mean ± SE arbitrary densitometric units. *, $P < 0.05$ versus human never smokers (B) or unexposed mice (C). The blot shown is representative of two experiments (A), or the data are the mean from the number of human subjects (B) or mice (C) indicated.

demonstrated a time-dependent decline in SOCS3 levels in BALF that was dramatic by day 7 (Fig. 8 C). Together, these data in humans and mice document a substantial impairment in the in vivo secretion of SOCS proteins in the alveolar space in association with the known inflammatory response that characterizes cigarette smoke exposure.

DISCUSSION

Here we have demonstrated that AMs from humans and rodents constitutively secrete SOCS1 and SOCS3 proteins, the best-studied members of the SOCS family, and that relevant bioactive molecules can tune secretion up or down within minutes. SOCS1 and -3 are secreted within specific types of vesicles, namely Exos and MPs, respectively, which can be taken up by AECs to inhibit cytokine-induced STAT activation in vitro and in vivo. SOCS proteins are arguably the most important brakes on intracellular cytokine signaling, but to our knowledge they have never previously been identified in the extracellular space in any cell, tissue, or context. The finding that secreted SOCS proteins can serve as vectors mediating macrophage to epithelial cell cross-talk thus represents a new paradigm for the control of inflammatory and immune responses. An important objective of future research will be to determine the role of this new mechanism in governing more biologically relevant forms of inflammation, such as infection and smoking; such work will need to account for the bidirectional interactions between AMs and AECs occurring over distinct time frames.

SOCS1 and SOCS3 thus join a growing list of diverse molecules once thought to be exclusively intracellular but now recognized to be secreted via unconventional, often vesicular, pathways. Although MPs and Exos derive from distinct cellular membranes, they often harbor overlapping cargo (Choi et al., 2013). Little is known about vesicular secretion in macrophages, and we are aware of only one report of Exos secretion (Bernard et al., 2014) and no reports of MP secretion in AMs. SOCS1 and SOCS3 proteins were trafficked in AMs largely through different types of vesicles; however, because both types of vesicle undergo uptake by target cells with intracellular delivery of cargo molecules, as reflected by the ability of both AM-derived MPs and Exos to inhibit STAT activation, the functional significance of these divergent vesicular trafficking pathways is not clear at this time.

We identified two distinct mechanisms by which SOCS3 protein secretion could be rapidly modulated. First, macrophage adherence to culture dishes triggered a burst of secretion of SOCS3 that paralleled a burst in MP release. This pattern of increased secretion owing to increased MP release is similar to that which has been well delineated for secretion of tissue factor by platelets and endothelial cells during vascular injury (Mallat et al., 2000). The second form of modulation was characterized by rapid changes in SOCS3 secretion, increases in response to both PGE_2 and IL-10 but decreases in response to LPS, in the absence of changes in the number of MPs released. This form of regulated secretion appears to reflect differential packaging or sorting of SOCS3 into vesicles. Mechanisms responsible for such sorting, especially of cytosolic proteins, are not well understood (Raposo and Stoorvogel, 2013), but various forms of lipidation that target proteins to particular membrane microdomains may be involved (Shen et al., 2011). Determining the mechanisms by which packaging of SOCS proteins into MPs and Exos can be differentially regulated by pro- and antiinflammatory substances must await a better understanding of the fundamental molecular basis for

vesicular protein sorting. In any case, it is of teleological interest that PGE_2 and IL-10 potentiated, whereas LPS inhibited, basal macrophage SOCS secretion, and it is intriguing to speculate that their opposing effects on this process may contribute to the antiinflammatory actions of the former and the proinflammatory actions of the latter. The signaling mechanisms by which these distinctive effects on SOCS secretion are realized also remain to be defined.

Robust SOCS secretion during adherence and culture was a conserved property of resident AMs from various mammalian species. That this was also operative in vivo was suggested by the very high concentration of immunoreactive SOCS3 in BALF of naive mice (~10 ng/ml). This level is substantially higher than the usual range of 10–200 pg/ml observed for most cytokines and was even higher than the 0.5–1 ng/ml level noted for GM-CSF, which is itself known to be particularly enriched in the pulmonary alveolar compartment (Guth et al., 2009). These results are suggestive of an important role for SOCS proteins in alveolar homeostasis.

In contrast, SOCS secretion was far less evident in a variety of nonpulmonary macrophage populations. Abundant expression of SOCS proteins would seem to be a prerequisite for their secretion, but it is clearly not sufficient, as indicated by the pattern in lung fibroblasts (Fig. 6 E). Resident peritoneal and spleen macrophages as well as differentiated U937 cells neither expressed nor secreted appreciable levels of SOCS3, and future studies will be required to determine whether these cell types truly lack the capacity for secretion under circumstances where expression is not limiting. Nevertheless, their low level of SOCS expression relative to AMs has not, to our knowledge, been previously recognized either. We speculate that greater expression of SOCS proteins in AMs reflects transcriptional up-regulation dictated by substances that are particularly abundant in the alveolar milieu, such as GM-CSF (Guth et al., 2009). Although the high levels of expression and secretion of SOCS3 noted in bone marrow–derived macrophages suggests that macrophages from sites other than the lung may have the capacity to manifest SOCS secretion under the proper circumstances, the fact that these cells were differentiated by in vitro culture in the presence of high concentrations of M-CSF makes their relevance to organ-resident macrophages uncertain. In any case, abundant expression and secretion of SOCS proteins, as demonstrated herein, may represent a previously unrecognized determinant of the unusual quiescent and suppressive aspects, respectively, of the AM phenotype.

Because they comprise the enormous air–lung interface and are the immediate neighbors of AMs, AECs are logical targets for the actions of AM-secreted SOCS proteins. We assessed their biological responses to vesicular SOCS by administering vesicles in vitro and in vivo and using as negative controls vesicles from macrophages with a relative lack of SOCS (derived either from AMs subjected to siRNA-mediated knockdown or from PMs). Both in vitro and in vivo models clearly demonstrated that AM-derived SOCS proteins indeed dampen inflammatory responses in AECs. Further investigation will be required to explore the possibility that other resident or recruited cells in the alveolar space, such as lymphocytes and dendritic cells, might also be targeted by AM-derived SOCS. However, AEC acquisition of biologically active SOCS3 from donor AMs may be particularly meaningful because AECs themselves expressed negligible levels of this protein (Fig. 6 F). This finding is consistent with a recent immunohistochemical analysis of normal human lung that found in situ SOCS3 staining to be ~30-fold lower in AECs than in AMs (Akram et al., 2014). Beyond the lung, a survey of inflamed human tissues has noted a lower degree of immunostaining for SOCS3 in a variety of epithelia than in leukocytes (White et al., 2011), and human keratinocytes have been reported to manifest lower basal and inducible expression of SOCS3 than do autologous monocyte-derived macrophages (Zeitvogel et al., 2012). In view of these observations, it has been suggested that a relatively low abundance of SOCS3 in epithelia may be important to permit adequate proliferative capacity of epithelial cells during repair responses (Zeitvogel et al., 2012). The distinctive capacity of AMs to abundantly express and secrete SOCS proteins may therefore represent an adaptation designed to compensate for deficient SOCS within the cells constituting the surface of the hostile pulmonary milieu, and thereby restrain inflammatory responses via cell–cell cooperation. Furthermore, the ability of AECs to elaborate substances such as PGE_2 and IL-10 may endow them with the means to rapidly "request" SOCS from AMs, completing a bidirectional circuit that favors the restoration of homeostasis at the alveolar surface.

Although cigarette smoking is well known to be associated with an increase in the number and activation state of AMs in the lung (Holt, 1987; Cosio et al., 2009), SOCS secretion was diminished in BALF in normal humans and mice exposed to cigarette smoke. This finding suggests that the amplitude of SOCS secretion may represent a previously unrecognized determinant of early smoking-induced inflammatory events. BALF levels of SOCS proteins may therefore have utility as biomarkers, much as has been established for circulating levels of vesicular proteins in vascular disease (Wang et al., 2013). As SOCS3 expression has been reported to be similar between AM lysates of healthy human smokers and nonsmokers (Dhillon et al., 2009), the reduction in BALF levels of SOCS3 in smokers likely reflects a decrease in its secretion by AMs. This, in turn, could reflect either the inhibitory effects on SOCS secretion of the high levels of LPS found in cigarette smoke (Hasday et al., 1999) or impaired secretion in smokers caused by a relative deficiency of secretagogues such as PGE_2 (Balter et al., 1989) and IL-10 (Takanashi et al., 1999).

Exogenous administration of a form of SOCS3 engineered with a lipid tail to permit cell permeability was previously reported to inhibit STAT1 activation in vitro as well as in various animal models of inflammation in vivo (Jo et al., 2005). The secretion of vesicular SOCS by AMs thus represents a physiological parallel of that exogenous therapeutic intervention. Because SOCS proteins also regulate innate and adaptive immunity (Alexander and Hilton, 2004), cellular differentiation (Yoshimura et al., 1995) and survival (Duval

et al., 2000), hormone action (Greenhalgh and Alexander, 2004), and tumorigenesis (Alexander and Hilton, 2004), their secretion and transcellular delivery may have broad relevance and therapeutic potential.

MATERIALS AND METHODS

Animals. Pathogen-free 125–150 g female Wistar rats from Charles River and male C57BL/6 wild-type mice purchased from The Jackson Laboratory were used. Animals were treated according to National Institutes of Health (NIH) guidelines for the use of experimental animals with the approval of the University of Michigan Committee for the Use and Care of Animals.

Human subjects and BAL. Experiments were performed under a protocol approved by the Institutional Review Board of the VA Ann Arbor Healthcare System and registered at ClinicalTrials.gov as NCT01099410; all subjects gave written informed consent. Flexible fiberoptic bronchoscopy and BAL were performed on seven healthy volunteer subjects who were never smokers (age 44.4 ± 4.7 yr) and seven healthy current smokers (age 51.1 ± 2.8 yr; 20 ± 2.8 pack-years) with no respiratory symptoms or lung function abnormalities. Cell-free BALF was obtained after pelleting macrophages and was stored at −80°C.

Reagents. RPMI 1640 and F12-K were purchased from Gibco-Invitrogen. PGE_2 from Cayman Chemical was dissolved in DMSO and stored under N_2 at −80°C. Murine and rat cytokines (IL-6, IFNγ, and IL-10) were purchased from PeproTech. Mouse monoclonal Ab against SOCS3 and rabbit polyclonal Ab against SOCS1 were from Abcam and Cell Signaling Technology, respectively. Mouse monoclonal Ab against β-actin was from Sigma-Aldrich. FITC-conjugated rabbit polyclonal Abs against SOCS3 and SOCS1 were from Biorbyt. The fluorescent lipid 1-oleoyl-2-{6-[(7-nitro-2-1,3-benzoxadiazol-4-yl)amino]hexanoyl}-sn-glycero-3-phosphocholine (18:1-06:0 NBD PC) was purchased from Avanti Polar Lipids, Inc. Rabbit polyclonal Abs against phospho- and total STAT1 and STAT3 were from Cell Signaling Technology. LPS, monensin, hematoxylin, and proteinase K were from Sigma-Aldrich. Trypsin enzymatic antigen retrieval solution was from Abcam. Compounds requiring reconstitution were dissolved in PBS, EtOH, or DMSO. Required dilutions of all compounds were prepared immediately before use, and equivalent quantities of vehicle were added to the appropriate controls. DMSO or EtOH at the concentrations used had no direct effect on SOCS3 secretion.

Macrophage isolation and culture. Human AMs were obtained as described above. Resident AMs and PMs from rats and mice were obtained by lavage of the lung or the peritoneal cavity, respectively. Cells were resuspended in RPMI 1640 to a final concentration of $1–3 \times 10^6$ cells/ml. Cells were allowed to adhere to tissue culture–treated plates for at least 1 h (37°C, 5% CO_2), resulting in >99% of adherent cells identified as macrophages by use of modified Wright-Giemsa stain (Diff-Quick) from American Scientific Products. Rat bone marrow–derived macrophages were obtained from bone marrow cells cultured as described previously (Canetti et al., 2006) for 6 d in 100-mm-diameter Petri dishes in 30% L929 cell supernatant in RPMI 1640 containing 20% FCS, L-glutamine, and penicillin/streptomycin. After 3 d, the cell culture was supplemented with new medium totaling 50% of original volume. Spleens from C57BL/6 mice were minced and passed through a 40-µm filter (BD) to obtain a single cell suspension. Erythrolysis was performed with 10 ml of 0.8% ammonium chloride lysis buffer. Subsequently, cells were rinsed with HBSS and PBS/2 mM EDTA/0.5% FCS, followed by incubation with CD16/32 for 15 min at 4°C to avoid nonspecific binding of Abs. Cells were subsequently stained with F4/80 Ab for 15 min in 4°C, washed, and flow sorted to high purity (>96%).

Cell lines. The following cell lines were obtained from ATCC: (a) rat AEC lines L2 (CCL-149) and RLE-6TN (CRL-2300), spontaneously immortalized lines derived from primary cultures of adult rat AECs; (b) MH-S (CRL-2019), a line derived by SV40 transformation of primary murine AMs; (c) NR8383 (CRL-2192), a line derived by spontaneous transformation of primary rat AMs; (d) normal human adult lung fibroblasts (CCL-210); and (e) U937 cells (CRL-1593), myelomonocytic leukemia cells which were used after differentiation into macrophage-like cells by 100 nM phorbol myristate acetate treatment for 16 h.

RNA isolation and quantitative RT-PCR (qRT-PCR) determination of mRNA levels of MCP-1. RNA was extracted using QIAGEN columns according to the manufacturer's instructions and converted to cDNA. MCP-1 mRNA levels were assessed by qRT-PCR performed with a SYBR Green PCR kit (Applied Biosystems) on an ABI Prism 7300 thermocycler (Applied Biosystems). The sequences of the primers used for MCP-1 and β-actin amplification, respectively, were 5′-AGCATCCACGTGTTGGCTC-3′ (f), 5′-CCAGCCTACTCATTGGGATCAT-3′ (r) and 5′-ACCCTAAGGCCAACCGTGA-3′ (f), 5′-CAGAGGCATACAGGGACAGCA-3′ (r). Relative gene expression was determined by the ΔCT method, and β-actin was used as a reference gene. Primer efficiency tests were performed on all primers and ranged from 97% to 107%.

Western blotting. AMs ($3–4 \times 10^6$) were plated in 6-well tissue culture dishes and incubated in the presence or absence of compounds of interest for the indicated amounts of time. Then supernatants were harvested (4 ml) and centrifuged at 500 *g* (10 min) and 2,500 *g* (10 min) to yield CM. Secreted proteins were concentrated using 3 kD Amicon size exclusion filters from EMD Millipore, after an aliquot (150 µl) was kept for LDH assay. Protein concentrations were determined by the DC protein assay (modified Lowry protein assay) from Bio-Rad Laboratories. Samples containing 30 µg protein were separated by SDS-PAGE using 12% gels and then transferred overnight to nitrocellulose membranes. After blocking with 4% BSA, membranes were probed overnight with commercially available Abs directed against SOCS (titer of 1:500), phospho- and total STAT (titer of 1:1,000), and β-actin (titer of 1:10,000). After incubation with peroxidase-conjugated goat anti–rabbit (or anti–mouse) secondary Ab (titer of 1:10,000) from Cell Signaling Technology, film was developed using ECL detection from GE Healthcare. Relative band densities were determined by densitometric analysis using NIH ImageJ software, and relative band densities for experimental conditions were expressed as described in the figure legends.

Detection of SOCS3 by ELISA. A commercially available ELISA kit (Cloud-Clone) was used to quantify SOCS3 levels in AEC lysates or in BALF sonicated (Branson Sonifier 250; 40% duty cycle, output 3) for 10 s on ice three times to disrupt MPs.

Detection of TNF by ELISA. TNF was measured in the cell culture supernatant from AMs plated in 96-well plates at a density of 0.5×10^6 cells/100 µl. Supernatants were collected after 1 h, cell debris was removed by centrifugation (500 *g*, 10 min), and samples were analyzed by immunoassay kits from R&D Systems.

Cytotoxicity. Leakage of cytosolic proteins was assessed by cytotoxicity detection kit (LDH) from Roche Diagnostics. AMs were cultured and supernatants were centrifuged for 10 min at 500 *g* and 2,500 *g*, and then LDH release assay was performed.

Purification of MPs and Exos. Rat AMs were cultured as described in Macrophage isolation and culture, and the culture supernatant was harvested for the enrichment of MPs (Brogan et al., 2004) and Exos (Théry et al., 2006). In brief, CM obtained from AM supernatants as described above was centrifuged at 17,000 *g* for 160 min. The final pellets were resuspended in 200 µl of Ca^{2+}-free Tyrode's buffer for flow cytometric analysis or resuspended in RPMI 1640 for in vitro studies or PBS for in vivo studies, while the remaining supernatants were further enriched for Exos by ultracentrifugation at 100,000 *g* at 4°C for 90 min.

Flow cytometry analysis. Flow cytometry was performed using a BD FACSCanto 2. MPs were incubated with annexin V–FITC or FITC control

from BD for 20 min at room temperature in the dark. Then samples were permeabilized with 0.2% NP-40 and incubated with 0.5 µg FITC-conjugated SOCS3 Ab. The light scatter and fluorescence channels were set at logarithmic gain. Calibration of MP size was performed using a Polybead Sampler kit from Polysciences, Inc. Samples were immediately analyzed by flow cytometry. Using 1.0-µm beads as standard, we quantified the number of MPs in known volumes of the MP aliquot. 10,000 events were acquired for each sample. For MP quantification, up to 25,000 events were acquired. Data were analyzed using FlowJo software (BD).

AM and MP staining and microscopy. To label plasma membranes, AMs were incubated with 100 µM of the fluorescent lipid 18:1-06:0 NBD PC for 20 min on ice in the dark and then washed three times before plating them. Slides were mounted in SlowFade Gold antifade mounting media with DAPI (Molecular Probes) to visualize nuclei. Cells were imaged on a Nikon Eclipse E600 Microscope (magnification 100).

For MPs, rat AMs were cultured in RPMI without Phenol red, and then AM supernatant was harvested and processed for the enrichment of MPs, as described above. MPs were incubated with annexin V–FITC from BD for 20 min at room temperature in the dark and were imaged on a Nikon TE300 with a 60× oil immersion objective (NA 1.40, total magnification of 600).

RNA interference. RNA interference was performed according to a protocol provided by GE Healthcare. Rat AMs were transfected using Lipofectamine RNAiMax reagent from Invitrogen with 100 nM nontargeting SMARTpool control or specific ON-TARGET SMARTpool SOCS3 and SOCS1 siRNA from GE Healthcare. After 72 h of transfection, AMs were washed and incubated for 48 h with RPMI 1640.

In vitro transfer experiments. To assess the uptake and functional effects of secretory products of rat AMs in recipient rat AECs, AECs were incubated with F12-K medium or CM, at either 37°C or 4°C for times ranging from 30 min to 2 h. Alternatively, they were incubated with either MPs or Exos isolated from AM-derived CM or with CM that had been depleted of MPs by centrifugation. SOCS3 transfer was determined after a 2-h incubation with AM-derived CM by quantifying immunoreactive SOCS3 in AEC lysates using ELISA. Uptake of MPs was determined by labeling MPs with annexin V–FITC, as described above, incubating them with AECs for 1 h at a ratio of 10:1, and determining fluorescence in AECs by flow cytometry after trypsinization and washing. To evaluate modulation of STAT activation, AECs were pretreated with CM, MP-depleted CM, MPs, or Exos before treatment with IL-6 (20 ng/ml) or IFNγ (5 ng/ml) for 1 h. Inhibition of IL-6–induced STAT3 and IFNγ-induced STAT1 activation was assessed by WB using Abs directed against Tyr705 phospho-STAT3 and Tyr701 phospho-STAT1, respectively. The contribution of SOCS3 to inhibition of IL-6–induced STAT3 or IFNγ-induced STAT1 activation was determined by comparing the inhibitory ability of CM obtained from AMs pretreated for 3 d with SOCS3 versus control siRNA. SOCS3 knockdown in cell lysates and CM was evaluated by WB.

Mouse model of cigarette smoke exposure. 8–10-wk-old female C57BL/6 mice were exposed for 2 h/d for 3 or 7 d to mainstream cigarette smoke from research cigarettes, as described previously (Phipps et al., 2010); control mice were unexposed. BALF was obtained after sacrifice and analyzed for SOCS1 and -3 content by WB. The number of mice available for analysis per group is shown in the figures.

In vivo experiments. Levels of SOCS3 and SOCS1 in concentrated BALF from naive or smoked mice or healthy human never smokers and current smokers were determined by WB and/or ELISA. To evaluate the ability of immunomodulatory substances to influence BALF levels of SOCS3, mice were subjected to oropharyngeal administration into the lungs of 50 µl saline containing 15 µg PGE_2 and/or LPS or vehicle alone. BALF was harvested 3 h later and analyzed by WB for SOCS3. For in vivo transfer experiments, MPs from rat AMs and PMs were isolated and quantified using flow cytometry, and 3×10^6 MPs were oropharyngeally administered per mouse. 2 h later, 0.1 µg IFNγ was administered by the same route. Responses analyzed 1 h thereafter in lung homogenates after initial lung lavage to remove AMs included Tyr701 phospho-STAT1 and Tyr705 phospho-STAT3 by WB, MCP-1 mRNA determination by qRT-PCR, and immunostaining (see below).

Immunohistochemical staining and image analysis of lung sections. Lungs were harvested from mice treated as described above, fixed in formalin, and processed as previously described (Brock et al., 2001). A trypsin enzymatic antigen retrieval solution was applied for 15 min at room temperature. Rabbit polyclonal Abs against phospho-STAT1 (titer 1:50) were applied overnight at 4°C. Nuclei were briefly counterstained with hematoxylin after completion of immunostaining. Images were taken using a Nikon Eclipse E600 Microscope (magnification 40). p-STAT1 staining was quantified by first separating the colors using color deconvolution plugin (ImageJ software) and performing densitometric analysis of red staining in 10 randomly selected fields, which was expressed relative to the area of the whole field.

Statistical analysis. The data are presented as mean ± SEM. Most are derived from three or more independent experiments and were analyzed with the Prism 5.0 statistical program from GraphPad Software; in instances where fewer experiments were performed, it is mentioned in the figure legend. The group means for different treatments were compared either by ANOVA with significance determined by Bonferroni or by Student's *t* test analysis. Statistical significance was set at a p-value <0.05.

We thank Samuel W. Straight, Aminul Islam, Sarah Akhtar, and Hannah Feather for their technical assistance and the members of the Peters-Golden laboratory for helpful input, as well as Richard H. Simon, Steven Huang, and Peter A. Ward for reading the manuscript.

This work was supported by National Institutes of Health grants HL058897 (to M. Peters-Golden) and HL082480 (to J.L. Curtis); by Merit Review Award BX001389 (to C.M. Freeman) and Research Enhancement Award Program (REAP) funding (to J.L. Curtis) from the Biomedical Laboratory Research and Development Service, Department of Veterans Affairs; by FAMRI CIA-103071 (to P. Mancuso); and by American Lung Association Senior Research Training Fellowships (to E. Bourdonnay and Z. Zasłona). Data came from trials registered by ClinicalTrials.gov as NCT00281190, NCT00281203, and NCT01099410.

The authors declare no competing financial interests.

Author contributions: E. Bourdonnay designed the research; performed experiments; collected, analyzed, and interpreted data; and wrote the manuscript. Z. Zasłona, L.R.K. Penke, and J.M. Speth performed experiments, analyzed data, and wrote the manuscript. S. Przybranowski, D.J. Schneider, and J.A. Swanson performed experiments and analyzed data. P. Mancuso, C.M. Freeman, and J.L. Curtis collected samples and wrote the manuscript. M. Peters-Golden supervised the work, designed research, analyzed data, and wrote the manuscript.

Submitted: 29 August 2014
Accepted: 17 March 2015

REFERENCES

Akram, K.M., N.J. Lomas, N.R. Forsyth, and M.A. Spiteri. 2014. Alveolar epithelial cells in idiopathic pulmonary fibrosis display upregulation of TRAIL, DR4 and DR5 expression with simultaneous preferential over-expression of pro-apoptotic marker p53. *Int. J. Clin. Exp. Pathol.* 7: 552–564.

Alexander, W.S., and D.J. Hilton. 2004. The role of suppressors of cytokine signaling (SOCS) proteins in regulation of the immune response. *Annu. Rev. Immunol.* 22:503–529. http://dx.doi.org/10.1146/annurev.immunol.22.091003.090312

Aronoff, D.M., C. Canetti, and M. Peters-Golden. 2004. Prostaglandin E_2 inhibits alveolar macrophage phagocytosis through an E-prostanoid 2 receptor-mediated increase in intracellular cyclic AMP. *J. Immunol.* 173:559–565. http://dx.doi.org/10.4049/jimmunol.173.1.559

Balter, M.S., G.B. Toews, and M. Peters-Golden. 1989. Multiple defects in arachidonate metabolism in alveolar macrophages from young asymptomatic smokers. *J. Lab. Clin. Med.* 114:662–673.

Bendtsen, J.D., L.J. Jensen, N. Blom, G. Von Heijne, and S. Brunak. 2004a. Feature-based prediction of non-classical and leaderless protein secretion. *Protein Eng. Des. Sel.* 17:349–356. http://dx.doi.org/10.1093/protein/gzh037

Bendtsen, J.D., H. Nielsen, G. von Heijne, and S. Brunak. 2004b. Improved prediction of signal peptides: SignalP 3.0. *J. Mol. Biol.* 340:783–795. http://dx.doi.org/10.1016/j.jmb.2004.05.028

Bernard, M.A., H. Zhao, S.C. Yue, A. Anandaiah, H. Koziel, and S.D. Tachado. 2014. Novel HIV-1 miRNAs stimulate TNFα release in human macrophages via TLR8 signaling pathway. *PLoS ONE.* 9:e106006. http://dx.doi.org/10.1371/journal.pone.0106006

Bourdonnay, E., C.H. Serezani, D.M. Aronoff, and M. Peters-Golden. 2012. Regulation of alveolar macrophage p40phox: hierarchy of activating kinases and their inhibition by PGE_2. *J. Leukoc. Biol.* 92:219–231. http://dx.doi.org/10.1189/jlb.1211590

Brandes, M.E., and J.N. Finkelstein. 1989. Stimulated rabbit alveolar macrophages secrete a growth factor for type II pneumocytes. *Am. J. Respir. Cell Mol. Biol.* 1:101–109. http://dx.doi.org/10.1165/ajrcmb/1.2.101

Brock, T.G., E. Maydanski, R.W. McNish, and M. Peters-Golden. 2001. Co-localization of leukotriene a4 hydrolase with 5-lipoxygenase in nuclei of alveolar macrophages and rat basophilic leukemia cells but not neutrophils. *J. Biol. Chem.* 276:35071–35077. http://dx.doi.org/10.1074/jbc.M105676200

Brogan, P.A., V. Shah, C. Brachet, A. Harnden, D. Mant, N. Klein, and M.J. Dillon. 2004. Endothelial and platelet microparticles in vasculitis of the young. *Arthritis Rheum.* 50:927–936. http://dx.doi.org/10.1002/art.20199

Canetti, C., D.M. Aronoff, M. Choe, N. Flamand, S. Wettlaufer, G.B. Toews, G.H. Chen, and M. Peters-Golden. 2006. Differential regulation by leukotrienes and calcium of Fcγ receptor-induced phagocytosis and Syk activation in dendritic cells versus macrophages. *J. Leukoc. Biol.* 79:1234–1241. http://dx.doi.org/10.1189/jlb.0705374

Chauncey, J.B., M. Peters-Golden, and R.H. Simon. 1988. Arachidonic acid metabolism by rat alveolar epithelial cells. *Lab. Invest.* 58:133–140.

Choi, D.S., D.K. Kim, Y.K. Kim, and Y.S. Gho. 2013. Proteomics, transcriptomics and lipidomics of exosomes and ectosomes. *Proteomics.* 13:1554–1571. http://dx.doi.org/10.1002/pmic.201200329

Chuquimia, O.D., D.H. Petursdottir, M.J. Rahman, K. Hartl, M. Singh, and C. Fernández. 2012. The role of alveolar epithelial cells in initiating and shaping pulmonary immune responses: communication between innate and adaptive immune systems. *PLoS ONE.* 7:e32125. http://dx.doi.org/10.1371/journal.pone.0032125

Cosio, M.G., M. Saetta, and A. Agusti. 2009. Immunologic aspects of chronic obstructive pulmonary disease. *N. Engl. J. Med.* 360:2445–2454. http://dx.doi.org/10.1056/NEJMra0804752

Dhillon, N.K., W.J. Murphy, M.B. Filla, A.J. Crespo, H.A. Latham, and A. O'Brien-Ladner. 2009. Down modulation of IFN-γ signaling in alveolar macrophages isolated from smokers. *Toxicol. Appl. Pharmacol.* 237:22–28. http://dx.doi.org/10.1016/j.taap.2009.02.021

Duval, D., B. Reinhardt, C. Kedinger, and H. Boeuf. 2000. Role of suppressors of cytokine signaling (Socs) in leukemia inhibitory factor (LIF) -dependent embryonic stem cell survival. *FASEB J.* 14:1577–1584. http://dx.doi.org/10.1096/fj.14.11.1577

Gasser, O., C. Hess, S. Miot, C. Deon, J.C. Sanchez, and J.A. Schifferli. 2003. Characterisation and properties of ectosomes released by human polymorphonuclear neutrophils. *Exp. Cell Res.* 285:243–257. http://dx.doi.org/10.1016/S0014-4827(03)00055-7

Greenhalgh, C.J., and W.S. Alexander. 2004. Suppressors of cytokine signalling and regulation of growth hormone action. *Growth Horm. IGF Res.* 14:200–206. http://dx.doi.org/10.1016/j.ghir.2003.12.011

Guth, A.M., W.J. Janssen, C.M. Bosio, E.C. Crouch, P.M. Henson, and S.W. Dow. 2009. Lung environment determines unique phenotype of alveolar macrophages. *Am. J. Physiol. Lung Cell. Mol. Physiol.* 296:L936–L946. http://dx.doi.org/10.1152/ajplung.90625.2008

Hasday, J.D., R. Bascom, J.J. Costa, T. Fitzgerald, and W. Dubin. 1999. Bacterial endotoxin is an active component of cigarette smoke. *Chest.* 115:829–835. http://dx.doi.org/10.1378/chest.115.3.829

Holt, P.G. 1987. Immune and inflammatory function in cigarette smokers. *Thorax.* 42:241–249. http://dx.doi.org/10.1136/thx.42.4.241

Hugel, B., M.C. Martínez, C. Kunzelmann, and J.M. Freyssinet. 2005. Membrane microparticles: two sides of the coin. *Physiology (Bethesda).* 20:22–27. http://dx.doi.org/10.1152/physiol.00029.2004

Hussell, T., and T.J. Bell. 2014. Alveolar macrophages: plasticity in a tissue-specific context. *Nat. Rev. Immunol.* 14:81–93. http://dx.doi.org/10.1038/nri3600

Hyde, D.M., N.K. Tyler, L.F. Putney, P. Singh, and H.J. Gundersen. 2004. Total number and mean size of alveoli in mammalian lung estimated using fractionator sampling and unbiased estimates of the Euler characteristic of alveolar openings. *Anat. Rec. A Discov. Mol. Cell. Evol. Biol.* 277A:216–226. http://dx.doi.org/10.1002/ar.a.20012

Jo, D., D. Liu, S. Yao, R.D. Collins, and J. Hawiger. 2005. Intracellular protein therapy with SOCS3 inhibits inflammation and apoptosis. *Nat. Med.* 11:892–898. http://dx.doi.org/10.1038/nm1269

John, G., K. Kohse, J. Orasche, A. Reda, J. Schnelle-Kreis, R. Zimmermann, O. Schmid, O. Eickelberg, and A.O. Yildirim. 2014. The composition of cigarette smoke determines inflammatory cell recruitment to the lung in COPD mouse models. *Clin. Sci.* 126:207–221. http://dx.doi.org/10.1042/CS20130117

Jose, P., M.G. Avdiushko, S. Akira, A.M. Kaplan, and D.A. Cohen. 2009. Inhibition of interleukin-10 signaling in lung dendritic cells by toll-like receptor 4 ligands. *Exp. Lung Res.* 35:1–28. http://dx.doi.org/10.1080/01902140802389727

Kelley, J.L., M.M. Rozek, C.A. Suenram, and C.J. Schwartz. 1987. Activation of human blood monocytes by adherence to tissue culture plastic surfaces. *Exp. Mol. Pathol.* 46:266–278. http://dx.doi.org/10.1016/0014-4800(87)90049-9

MacKenzie, A., H.L. Wilson, E. Kiss-Toth, S.K. Dower, R.A. North, and A. Surprenant. 2001. Rapid secretion of interleukin-1beta by microvesicle shedding. *Immunity.* 15:825–835. http://dx.doi.org/10.1016/S1074-7613(01)00229-1

Mallat, Z., H. Benamer, B. Hugel, J. Benessiano, P.G. Steg, J.M. Freyssinet, and A. Tedgui. 2000. Elevated levels of shed membrane microparticles with procoagulant potential in the peripheral circulating blood of patients with acute coronary syndromes. *Circulation.* 101:841–843. http://dx.doi.org/10.1161/01.CIR.101.8.841

Mause, S.F., and C. Weber. 2010. Microparticles: protagonists of a novel communication network for intercellular information exchange. *Circ. Res.* 107:1047–1057. http://dx.doi.org/10.1161/CIRCRESAHA.110.226456

Nicholson, S.E., T.A. Willson, A. Farley, R. Starr, J.G. Zhang, M. Baca, W.S. Alexander, D. Metcalf, D.J. Hilton, and N.A. Nicola. 1999. Mutational analyses of the SOCS proteins suggest a dual domain requirement but distinct mechanisms for inhibition of LIF and IL-6 signal transduction. *EMBO J.* 18:375–385. http://dx.doi.org/10.1093/emboj/18.2.375

Nickel, W., and C. Rabouille. 2009. Mechanisms of regulated unconventional protein secretion. *Nat. Rev. Mol. Cell Biol.* 10:148–155. http://dx.doi.org/10.1038/nrm2617

Phipps, J.C., D.M. Aronoff, J.L. Curtis, D. Goel, E. O'Brien, and P. Mancuso. 2010. Cigarette smoke exposure impairs pulmonary bacterial clearance and alveolar macrophage complement-mediated phagocytosis of Streptococcus pneumoniae. *Infect. Immun.* 78:1214–1220. http://dx.doi.org/10.1128/IAI.00963-09

Qing, Y., and G.R. Stark. 2004. Alternative activation of STAT1 and STAT3 in response to interferon-gamma. *J. Biol. Chem.* 279:41679–41685. http://dx.doi.org/10.1074/jbc.M406413200

Raposo, G., and W. Stoorvogel. 2013. Extracellular vesicles: exosomes, microvesicles, and friends. *J. Cell Biol.* 200:373–383. http://dx.doi.org/10.1083/jcb.201211138

Rubartelli, A., F. Cozzolino, M. Talio, and R. Sitia. 1990. A novel secretory pathway for interleukin-1 beta, a protein lacking a signal sequence. *EMBO J.* 9:1503–1510.

Sabat, R., G. Grütz, K. Warszawska, S. Kirsch, E. Witte, K. Wolk, and J. Geginat. 2010. Biology of interleukin-10. *Cytokine Growth Factor Rev.* 21:331–344. http://dx.doi.org/10.1016/j.cytogfr.2010.09.002

Sadallah, S., C. Eken, and J.A. Schifferli. 2008. Erythrocyte-derived ectosomes have immunosuppressive properties. *J. Leukoc. Biol.* 84:1316–1325. http://dx.doi.org/10.1189/jlb.0108013

Shen, B., N. Wu, J.M. Yang, and S.J. Gould. 2011. Protein targeting to exosomes/microvesicles by plasma membrane anchors. *J. Biol. Chem.* 286:14383–14395. http://dx.doi.org/10.1074/jbc.M110.208660

Standiford, T.J., S.L. Kunkel, M.A. Basha, S.W. Chensue, J.P. Lynch III, G.B. Toews, J. Westwick, and R.M. Strieter. 1990. Interleukin-8 gene expression by a pulmonary epithelial cell line. A model for cytokine networks in the lung. *J. Clin. Invest.* 86:1945–1953. http://dx.doi.org/10.1172/JCI114928

Starr, R., T.A. Willson, E.M. Viney, L.J. Murray, J.R. Rayner, B.J. Jenkins, T.J. Gonda, W.S. Alexander, D. Metcalf, N.A. Nicola, and D.J. Hilton. 1997. A family of cytokine-inducible inhibitors of signalling. *Nature.* 387:917–921. http://dx.doi.org/10.1038/43206

Takanashi, S., Y. Hasegawa, Y. Kanehira, K. Yamamoto, K. Fujimoto, K. Satoh, and K. Okamura. 1999. Interleukin-10 level in sputum is reduced in bronchial asthma, COPD and in smokers. *Eur. Respir. J.* 14: 309–314.

Tamiya, T., I. Kashiwagi, R. Takahashi, H. Yasukawa, and A. Yoshimura. 2011. Suppressors of cytokine signaling (SOCS) proteins and JAK/STAT pathways: regulation of T-cell inflammation by SOCS1 and SOCS3. *Arterioscler. Thromb. Vasc. Biol.* 31:980–985. http://dx.doi.org/10.1161/ATVBAHA.110.207464

Thepen, T., G. Kraal, and P.G. Holt. 1994. The role of alveolar macrophages in regulation of lung inflammation. *Ann. N. Y. Acad. Sci.* 725:200–206. http://dx.doi.org/10.1111/j.1749-6632.1994.tb39802.x

Théry, C., S. Amigorena, G. Raposo, and A. Clayton. 2006. Isolation and characterization of exosomes from cell culture supernatants and biological fluids. *Curr. Protoc. Cell Biol.* Chapter 3:Unit 3.22.

Wang, J.W., C.M. Gijsberts, A. Seneviratna, V.C. de Hoog, J.E. Vrijenhoek, A.H. Schoneveld, M.Y. Chan, C.S. Lam, A.M. Richards, C.N. Lee, et al. 2013. Plasma extracellular vesicle protein content for diagnosis and prognosis of global cardiovascular disease. *Neth. Heart J.* 21:467–471. http://dx.doi.org/10.1007/s12471-013-0462-3

Westphalen, K., G.A. Gusarova, M.N. Islam, M. Subramanian, T.S. Cohen, A.S. Prince, and J. Bhattacharya. 2014. Sessile alveolar macrophages communicate with alveolar epithelium to modulate immunity. *Nature.* 506:503–506. http://dx.doi.org/10.1038/nature12902

White, G.E., A. Cotterill, M.R. Addley, E.J. Soilleux, and D.R. Greaves. 2011. Suppressor of cytokine signalling protein SOCS3 expression is increased at sites of acute and chronic inflammation. *J. Mol. Histol.* 42:137–151. http://dx.doi.org/10.1007/s10735-011-9317-7

Yoshimura, A., T. Ohkubo, T. Kiguchi, N.A. Jenkins, D.J. Gilbert, N.G. Copeland, T. Hara, and A. Miyajima. 1995. A novel cytokine-inducible gene CIS encodes an SH2-containing protein that binds to tyrosine-phosphorylated interleukin 3 and erythropoietin receptors. *EMBO J.* 14:2816–2826.

Yoshimura, A., T. Naka, and M. Kubo. 2007. SOCS proteins, cytokine signalling and immune regulation. *Nat. Rev. Immunol.* 7:454–465. http://dx.doi.org/10.1038/nri2093

Zeitvogel, J., A. Dalpke, B. Eiz-Vesper, M. Kracht, O. Dittrich-Breiholz, T. Werfel, and M. Wittmann. 2012. Human primary keratinocytes show restricted ability to up-regulate suppressor of cytokine signaling (SOCS)3 protein compared with autologous macrophages. *J. Biol. Chem.* 287:9923–9930. http://dx.doi.org/10.1074/jbc.M111.280370